Bacterial Foraging Optimization Algorithm (BFOA) to Simulate Thermal Distribution in Yb:YAG Laser Thin Disk

Dr. Mohammed A.Minshed
Laser and Optoelectronics Engineering Department, University of Technology/Baghdad
Email: dr.mohhamedwhab@gmail.com

Received on: 3/4/2012 & Accepted on: 24/6/2012

ABSTRACT

There is a strong need for an optimized management of the thermal problem in Yb:YAG laser rod and for a powerful, fast, and accurate modeling tool capable of treating the heat source distribution very close to what it actually is. In this paper, a new optimization algorithm called Bacterial Foraging Optimization Algorithm (BFOA) is proposed for simulation of the radial heat distribution. A BFOA discloses a simulation method which delivers the exact temperature distribution in a circularly cylindrical structure with a circularly symmetrical, longitudinally, and transversally non-uniform heat source distribution and circularly symmetrical cooling means. its rod was end pumped with 940 nm and it has been tested with pump power ranging from 1Kw to 2Kw for radius pumping ratio of 1/2, 1/3, and 1/4, for both Top hat and Gaussian beam pumping . The output power is obtained and compared with previously published experimental measurements for different pump power and a good agreement has been found.

Keywords: Solid State Lasers, Thermal Distribution, Bacterial Foraging, Optimization Algorithm.

الخوارزمية البكتيرية الرياضية لمحاكاة التوزيع الحراري في ليزر Yb:YAG

الخلاصة

هناك حاجة قوية لأدارة مثلى لمشكلة الحرارة في ليزر Yb: YAG، النمذجة أداة سريعة ودقيقة قادرة على معالجة توزيع درجة الحرارة وقريبة جدا من ما هو عليه في الواقع. في هذا البحث، تم أستخام خوارزمية جديدة تسمى Bacterial Foraging Optimization Algorithm (BFOA)) يكشف أسلوب المحاكاة التي توفر توزيع درجات الحرارة بالضبط في شكل أسطواني متناظر يتم الحصول عليها ومقارنتها مع القياسات التجريبية المنشورة للوثوق بالنموذج الرياضي. وكان الطول الموجي المستخدم بالضخ هو ٩٤٠ نانومتر أما لمحاكاة التوزيع الحرارة. BFOA

https://doi.org/10.30684/etj.2013.71254
2412-0758/University of Technology-Iraq, Baghdad, Iraq

الطول الموجي الخارج هو ١٠٣٠ نانومتر. حدود القدرة المستخدمة في الضخ تراوحت مـــن(١ – ٢ Kw)). اما القدرة الخارجة تم مقارنتها بنتائج عملية منشورة سابقا حيث تم الحصول على نتائج ضمن الحدود المقبولة.

List of Symbol

$Q_p(r,t)$	the rate of energy generated from the absorbed part of the pump beam per unit volume,
$Q_L(r,z,t)$	the rate of energy generated from the absorbed part of the amplified laser radiation per unit volume
k	the thermal conductivity of the material
$T_L(r,z,t)$	the temperature distribution generated from the absorbed part of the amplified laser beam
$T_p(r,t)$	the temperature distribution generated from the absorbed pump radiation
$\alpha = k/(\rho C_p)$	the thermal diffusivity of the material
ρ	the mass density of the material,
C_p	is the specific heat of the material at constant pressure
h	and is the heat transfer coefficient
Q	is thermal factor

INTRODUCTION

Some new approaches and technical implementations have been proposed for diode pumped solid state lasers (DPSSL's), however, basically physics of the problem has remained the same. Typical routes of thermal effects control in DPSSL's can be divided into three groups [1]:

1- Improvement in gain media technology,
2- New designs of pumping schemes and resonators,
3- Improvement in cooling techniques.

The analytical expressions obtained for the temperature distribution open the way to a better physical understanding of thermal phenomena and represent a fast tool for solid-state laser design and optimization [2]. Optimization is associated with almost every problem of engineering. The underlying principle in optimization is to enforce constraints that must be satisfied while exploring as many options as possible within tradeoff space. There exists numerous optimization techniques. Bio-inspired or nature inspired optimization techniques are class of random search techniques suitable for linear and nonlinear process. Hence, nature based computing or nature computing is an

attractive area of research. Like nature inspired computing, their applications areas are also numerous. To list a few, the nature computing applications include optimization, data analysis, data mining, computer graphics and vision, prediction and diagnosis, design, intelligent control, and traffic and transportation systems. Most of the real life problem occurring in the field of science and engineering may be modeled as nonlinear optimization problems, which may be unimodal or multimodal. Multimodal problems are generally considered more difficult to solve because of the presence of several local and global optima. Bacterial Foraging Optimization proposed in 2002 by K.M. Passino is based on the foraging behavior of Escherichia Coli (E. coli) bacteria present in the human intestine [3]**.** There are many species of bacteria that evidently perform some type of optimization during their motile behavior. Some optimize their position based on other chemicals, and others based on non-chemcial stimuli (e.g. light, magnetism, or heat). Each of these holds the potential for the creation of a bioinspired optimization method [4].

TEMPERATURE DISTRIBUTION

The achievement of high power laser systems with high beam quality is largely compromised by thermal effects in the gain medium, which are responsible for thermal lensing, depolarization losses, and ultimately fracture [5]. The equations governing the temperature distribution are given by:

1) The heat diffusion equations in cylindrical coordinates

i- Originating from the pump beam

i- Originating from the pump beam

$$\frac{\partial^2 T_p(r,t)}{\partial r^2}+\frac{1}{r}\frac{T_p(r,t)}{\partial r}+\frac{1}{k}Q_p(r,t)=\frac{1}{\alpha}\frac{\partial T_p(r,t)}{\partial t} \qquad \dots (1)$$

ii- Originating from the laser radiation

$$\frac{\partial^2 T_L(r,z,t)}{\partial r^2}+\frac{1}{r}\frac{T_L(r,z,t)}{\partial r}+\frac{\partial^2 T_L(r,z,t)}{\partial z^2}+\frac{1}{k}Q_L(r,z,t)=\frac{1}{\alpha}\frac{\partial T_L(r,z,t)}{\partial t} \qquad \dots (2)$$

2) The boundary condition describing the cooling at the outer radius of

The rod.

$$-k\frac{\partial T_t(r,z,t)}{\partial r}\Big|_{r=R}=h\,T_t(r,z,t)\Big|_{r=R} \qquad \dots (3)$$

With $T_t(r,z,t)=T_L(r,z,t)+T_p(r,t)$

where $Q_p(r,t)$ is the rate of energy generated from the absorbed part of the pump beam per unit volume, $Q_L(r,z,t)$is the rate of energy generated from the absorbed part of the amplified laser radiation per unit volume, *k* is the thermal conductivity of the material, $T_L(r,z,t)$is the temperature distribution generated from the absorbed part of the amplified laser beam, $T_p(r,t)$ is the temperature distribution generated from the absorbed pump radiation, $\alpha = k/(\rho C_p)$ is the thermal diffusivity of the material; $\rho$is the mass density of the material, C_p is the specific heat of the material at constant pressure and *h* is the heat transfer coefficient [6].

For the quasi three-level system such as Yb: YAG, the temperature increase should be small enough because it can strongly populate the lower working level of Yb ion. Therefore, in such media the temperature rise must be controlled carefully. If the temperature increase does not significantly disturb the population of the lower working level of active media as is the case with Nd: YAG, the other effects can limit the performance of the laser. The most significant of these effects is a thermally induced change of the optical path difference (OPD). It is commonly assumed that the optical path difference is essentially proportional to the temperature rise $\Delta T$and can be found using formula [7].

$$OPD = \int \frac{dn}{dT} \Delta T \, dz \qquad \ldots (4)$$

Thermal effects play a major role in solid-state lasers, where they cause lensing and polarization coupling through built-in stress and strain fields. The modeling of the thermal problem has been an important issue as from the first days of laser science and technology [8]. Numerical modeling remains however a rather long exercise and suffers the usual limitation that there is no insurance of the correctness of the solution. This is why an analytical treatment of the thermal problem remains of interest. A further interest stems from the fact that a number of laser geometries, such as axially pumped systems, exhibit a circularly cylindrical symmetry, thus lending them to an easier analytical analysis. Moreover, a number of structures not showing circular symmetry but pumped axially or radially can be treated on the basis of the assumption of circularly cylindrical symmetry with a reasonably good approximation [2].

3. Source density heat

Two types of possible pumping method can be tested; Gaussian and Top hat beam distribution, they will cause heat generation through the laser medium. For Gaussian beam distribution, the heat generation through the laser medium ($Q(r,z)$ in W/m^2) can be written as:

$$Q(r,z) = \frac{2Q\mu \exp\left(\frac{-2r^2}{w_o^2}\right)\exp(-\mu z)}{\pi\, w_o^2\,[1-\exp(-\mu L)]} \qquad \ldots(5)$$

Where $Q=\eta P$,$\eta$is thermal factor, P absorption power(W), $w_o$waist radius (m), μ absorption coefficient (3.50), L is length of laser rod (m). For uniform power distribution through the beam (Top hat), the heat generation through the laser medium can be written as:

$$Q(r,z) = \frac{Q\mu \exp(-\mu z)}{\pi\, a^2[1-\exp(-\mu L)]} \qquad r \leq a \qquad \ldots(6)$$

where heat generation is zero elsewhere (i.e. the heat generation vanishes when the radius is greater than the pumping beam radius a) [9].

4.Bacterial Foraging Optimization Algorithm (BFOA)

Swarm intelligence is the study of computational systems inspired by the 'collective intelligence'. Collective Intelligence emerges through the cooperation of large numbers of homogeneous agents in the environment. Examples include schools of fish, flocks of birds, and colonies of ants. Such intelligence is decentralized, self-organizing and distributed throughout an environment.The Bacterial Foraging Optimization Algorithm belongs to the field of Bacteria Optimization Algorithms and Swarm Optimization, and more broadly to the fields of Computational Intelligence and Metaheuristics. The Bacterial Foraging Optimization Algorithm is inspired by the group foraging behavior of bacteria such as E.coli and M.xanthus. Specifically, the BFOA is inspired by the chemotaxis behavior of bacteria that will perceive chemical gradients in the environment (such as nutrients) and move toward or away from specific signals. Bacteria perceive the direction to food based on the gradients of chemicals in their environment. Similarly, bacteria secrete attracting and repelling chemicals into the environment and can perceive each other in a similar way. Using locomotion mechanisms (such as flagella) bacteria can move around in their environment, sometimes moving chaotically (tumbling and spinning), and other times moving in a directed manner that may be referred to as swimming. Bacterial cells are treated like agents in an environment, using their perception of food and other cells as motivation to move, and stochastic tumbling and swimming like movement to re-locate. Depending on the cell-cell interactions, cells may swarm a food source, and/or may aggressively repel or ignore each other.The information processing strategy of the algorithm is to allow cells to stochastically and collectively swarm toward optima. This is achievedthrough a series of three processes on a population of simulated cells: 1) 'Chemotaxis' where the cost of cells is derated by the proximity to othercells and cells move along the manipulated cost surface one at a time (themajority of the work of the algorithm), 2) 'Reproduction' where only those cells that performed well over their

lifetime may contribute to the next generation, and 3) 'Elimination-dispersal' where cells are discarded and new random samples are inserted with a low probability [10].

The Bacterial Foraging Optimization is based on foraging strategy of *E. coli* bacteria. The foraging theory is based on the assumption that animals obtain maximum energy nutrients 'E' in a supposed to be a small time 'T'. The basic Bacterial Foraging Optimization consists of three principal mechanisms; namely chemotaxis, reproduction and elimination-dispersal. The brief descriptions of these steps involved in Bacterial Foraging are presented below[10].

1. Chemotaxis

During chemotaxis, the bacteria climb the nutrient concentration, avoid noxious substances, and search for a way out the of neutral media. This process is achieved through swimming and tumbling. The bacteria usually take a tumble followed by a tumble, tumble followed by a run, or swim. This movement of bacteria in each chemotaxis step can be expressedas[10]:

$$\theta^i(j+1,K,l) = \theta^i(j,K,l) + C(i)\frac{\Delta(i)}{\sqrt{\Delta^T(i)\,\Delta(i)}} \qquad \dots(7)$$

Where $\theta^i(j,K,l)$ represents position vector of *i*-th bacterium, in *j*-thchemotaxis step, in *k*-th reproduction step and in *l*-th elimination and dispersal step.$C(i)$Shows the step size taken in the random direction specified by the tumble.Δ (*i*) depict the direction vector of the *j*-thchemotaxis step. When the bacterial movement is run or swim, Δ(*i*) is taken as same that was available in the last chemotaxis step; otherwise, Δ(*i*) is a random vector whose elements lie in (-1, 1).

2. Reproduction

Using Eq. (8), the health/fitness of the bacteria is calculated.

$$J^i_{health} = \sum_{j=1}^{Nc+1} J(i,j,k,l) \qquad \dots(8)$$

Where, *Nc* is the maximum step in a chemotaxis step. During reproduction, all bacteria are sorted in reverse order according to fitness values. The least healthy bacteria die and the rest healthiest bacteria each splits into two bacteria, which are placed in the same location in the search space. This makes the population of bacteria remains constant .The reproduction process of bacterial foraging aims to speed up the convergence suitable in static problems, but not in dynamic environment [10].

The elimination and dispersal events assist chemotaxis progress by placing the bacteria to the nearest required values. In BFO, the dispersion event happens after a certain number of reproduction processes. Each bacterium according to a fixed probability dispersed from their original position and move to best position within the search space. These events may prevent the local optima trapping but lead to disturb the optimization process. Elimination and dispersal helps to avoid premature convergence or, being trapped in local optima [3].

SOCIAL COMMUNICATION

In nature there is the social communication between Bacterium such that they are neither close together nor far away from each other. This is done by releasing the chemical by the Bacteria. The chemical signal can be either attractant or Repellent. If the chemical signal released by the particular Bacteria is attractant in nature, then nit attracts other Bacteria to come to its position. On the contrary if the chemical signal released by the particular Bacteria is Repellent in nature, it doesn't allow other Bacteria to come to its position. The social communication between Bacterium can be simulated using the modified objective function to be computed for the i_{th}position corresponding to the i_{th}position Bacteria as given below [10].

$$J_{mod}(X^i) = J(X^i) + J_{social}(X^i) \qquad \dots(9)$$

Where J_{mod} is the modified Objective function computed for the i_{th}position X^i corresponding to the i_{th}Bacteria?$J(X^i)$Is the actual objective function value computed for the i_{th}position X^i corresponding to the i_{th}Bacteria?$J_{social}(X^i)$is the attractant cum repellent signal computed for the i_{th}position X^i corresponding to the i_{th} Bacteria as displayed below.

$$Let\ d_{ij} = |\quad |X^i - X^j|\ |^2$$

$$J_{social}(X^i) = M(\sum_{j=1}^{N} e^{-Rd_{ij}} - \sum_{j=1}^{N} e^{-Ad_{ij}}) \qquad \dots(10)$$

Note that if the first term is reduced if distance between the i_{th}position and others are made large and hence it acts as the repellent signal. Similarly the second term $\sum_{j=1}^{N} e^{-Rd_{ij}}$ is reduced if the distance between the i_{th}position and others are made small and hence it acts as the attractant signal. 'R' is the Repellent factor and 'A' is the attractant factor [11].

HEURISTICS

1. The algorithm was designed for application to continuous function optimization problem domains.
2. Given the loops in the algorithm, it can be configured numerous ways to elicit different search behavior. It is common to have a large number of chemotaxis iterations, and small numbers of the other iterations.
3. The default coefficients for swarming behavior (cell-cell interactions) are as follows $d_{attract}$ = 0.1, $w_{attract}$= 0.2, $h_{repellent}$ = $d_{attract}$, and $w_{repellent}$ = 10.
4. The step size is commonly a small fraction of the search space, such as 0.1.

5. During reproduction, typically half the population with a low health metric are discarded, and two copies of each member from the first (high-health) half of the population are retained.
6. The probability of elimination and dispersal (P_{ed}) is commonly set quite large, such as 0.25. [12].

OUTPUT POWER

As high output power is required, just for instance for laser machining processes, and the output power of the laser oscillator is not great enough the radiation will be guided through an amplifier that has to be pumped. The radiation to be amplified and the pump radiation both heat the amplifier and this may lead to phase change, thermal stresses leading to cracks and variation of the refractive index and under circumstances to vary the plane form of the input and output surfaces of the amplifier. These effects may lead to damage the amplifier or varying the front surface of the radiation leading to inaccurate laser machining. To avoid these changes a pre-study of the spatial and temporal temperature distribution has to be carried out in linear and nonlinear medium. The results of this study will be later applied in equations concerning the thermal stresses, the results of which will be necessary to determine the variation of the refractive index. With the aid of Maxwell equations the wave propagation in such an optically deformed amplifier will be determined. From the obtained results it will be hoped to find a way to correct the front surface of the wave and so to increases the accuracy of laser machining [13]. The volumetric heating of the laser material by the absorbed pump radiation and surface cooling required for heat reduction leads to a non-uniform temperature distribution in the material. This results in a distortion of the laser beam due to a temperature- and stress-dependent variation of the index of refraction. Thermal stress induced birefringence and thermal lensing effects caused in rod-shaped materials have been a big issue for realizing high performance solid-state lasers [14]. The starting point for analyzing the thermal aspects of laser tissue interactions is to define and understand the system of interest. In the most general sense, a system is identified as that portion of the universe that is involved directly in a particular process. The remainder of the universe is called the environment. The system interacts with the environment across its boundary. These interactions are directly responsible for changes that occur to the state of the system. The boundary surface provides a locus at which interactions can be identified and accounted for so as to predict resulting changes that will occur to the system. The temporal boundary condition is generally defined in terms of a known temperature distribution within the system at a specific time, usually at the beginning of a process of interest. However, definition of the spatial boundary conditions is not so straight forward. There are three primary classes of spatial boundary conditions that are encountered most frequently. The thermal interaction with the environment at the physical boundary of the system may be described in terms of a defined temperature, heat flux, or convective process.

The simplest specification for each of these conditions is that it remains constant over time, which leads to the most simple mathematical expression for the boundary condition. However, if the actual process of interest precludes using a constant boundary condition, as may be encountered in biological applications, then a more complex specification is required that may require a numerical solution [15]. The laser output power P_{out} is related to the photon number φ by the simple relation:

$$P_{out} = \frac{\gamma 2}{2\gamma}(hv)\frac{\varphi}{\tau_c} = \frac{\gamma 2c}{2L_s}hv\varphi \qquad \ldots(11)$$

In fact, $(hv)\ \varphi/\tau\_c$ is the total EM energy lost in the cavity per unit time, and solely a fraction $\gamma 2/2\gamma$ of this power is available due to transmission through the output mirror. The corresponding output laser power can be then calculated from the following equation:

$$P_{out} = \eta_s\,(P_p - P_{th}) \qquad \ldots(12)$$

where
$\eta_s = \eta_p \eta_c \eta_q \eta_t$.

Equation above shows that, within the approximation made, a linear relation is obtained between the output power and the pump power. One can then define the slope efficiency of the laser as $\eta_s = dP_{out}/dP_p$. According to (12), η_s is given by the product of four contributions, the pump efficiency η_p, the output coupling efficiency $\eta_c = \gamma 2/2\gamma$, the laser quantum efficiency $\eta_q = (hv)/(hv_{mp})$ and the transverse efficiency η_t = Ab/A, where Ab = Va/l is the transverse mode area in the active medium and A the transverse pumping area. The slope efficiency of a laser may typically vary from less than 1% in low-efficiency lasers (such as in the HeNe laser) to 20–50% or even higher in high-efficiency lasers [5].

THRESHOLD PUMP POWER

Once the threshold value of the pump rate is calculated, we can readily obtain the corresponding threshold pump power. we get in fact the following expressions:

$$P_{th} = \left(\frac{\gamma}{\eta_p}\right)\left(\frac{hv_p}{\tau}\right)\left[\frac{\pi\left(w_o^2 + w_p^2\right)}{2\sigma_e}\right] \qquad \ldots(13)$$

which hold for longitudinal pumping. Note that, again for longitudinal pumping, the threshold pump power increases as w_o is increased because, as w_o increases, the

wings of the mode extend further into the less strongly pumped regions of the active medium [6].

COMPUTER SIMULATION AND RESULTS

The simulation has been used to obtained temperature distribution, displacement across continuous pumped Yb:YAG laser rod , its rod was end pumped with 940 nm and it has been tested with pump power ranging from 1Kw to 2Kw for radius pumping ratio of 1/2, 1/3, and 1/4, for both Top hat and Gaussian beam pumping . A Gaussian beam diameter of 300μm has been chosen. The pumping power at 1Kw and radius pumping ratio of 1/2 is shown in figure (1). It shows that Gaussian beam pumping with respect time. Where the pulse width of pumping equal to 1msec. The absorption power from the crystal is calculated from the relation$P_{abs} = 0.2\ P_{pump}$, and the absorption power is described in figure (2):

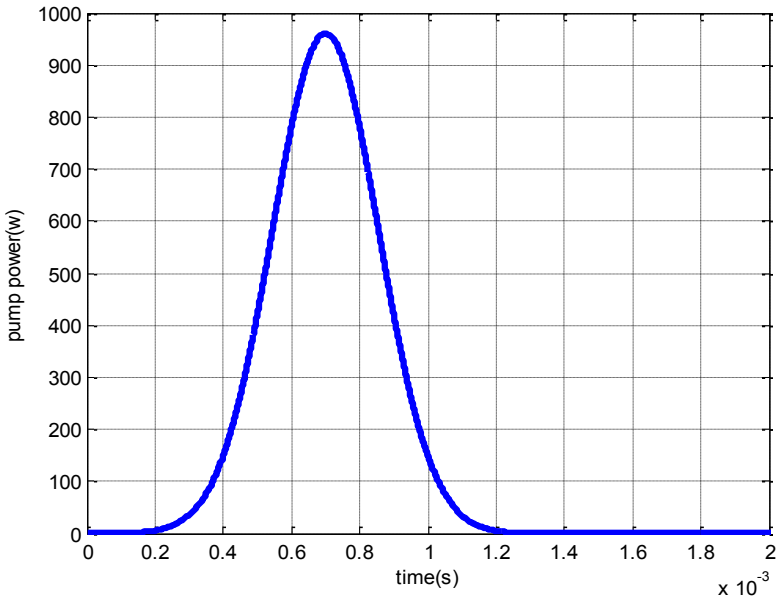

Figure (1) the output pump power from laser diode.

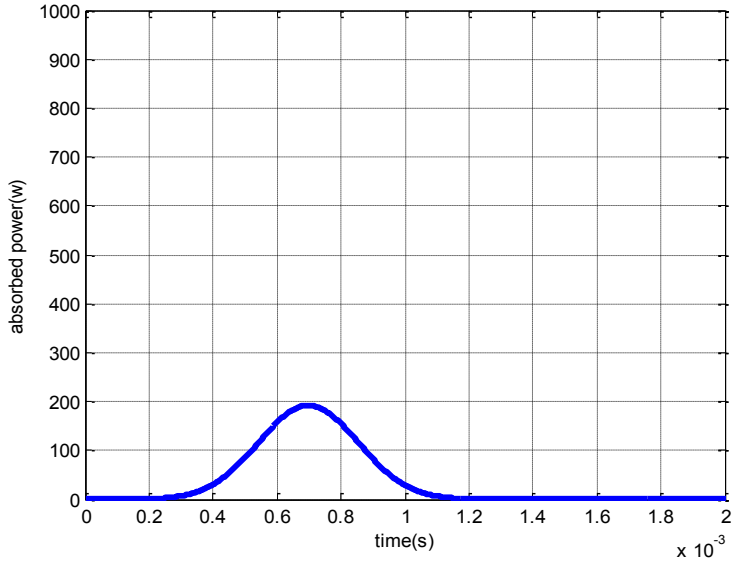

Figure (2) the absorption pump power.

Before presenting the results of bacterial swarm intelligence simulation, we discuss a simpler steady-state temperature distribution in symmetrical cylindrical rod with radially symmetric heating distributions. In this case Eq. (1) can be written as [6]:

$$\frac{1}{r}\left[k\frac{\partial}{\partial r}\left(r\frac{\partial T}{\partial r}\right)\right]+k\frac{\partial^2 T}{\partial z^2}+Q(r,z)=0 \qquad \ldots(14)$$

Where T is the temperature distribution in℃, $Q(r,z)$ is the heat source density that is function of the pump power density, r and z are the radial and longitudinal coordinates, k is the thermal conductivity of Yb:YAG laser rod. The Yb:YAG rod has a radius of 4mm and a length L of 250 μm. The heat transfer coefficients ($h_w = 0.67$ W. $\mathrm{cm}^{-2}.\mathrm{K}^{-1}$ and $h_a = 0.005$ W.$\mathrm{cm}^{-2}.\mathrm{K}^{-1}$) for the surfaces in contact with water and air, respectively. The total pump power of 80W has an absorption coefficient of 3.5cm^{-1}. The thermal conductivity of Yb:YAG is 13.0W. $\mathrm{m}^{-1}.\ \mathrm{K}^{-1}$. For Gaussian heat source the relation between thermal distribution and radius of laser rod is shown in figure (3). For Top hat heat source the relation between thermal distribution and radius of laser rod is shown in figure(4). Figure (5) represents the time dependence of the temperature induced by the pump beam calculated at any z value. The temperature increases as the irradiation time of the pump beam increases. It reaches its maximum value at t =1$m$sec which is greater than the time at which the intensity of the pump beam is maximum. Figure (6) represent the time dependence of

the temperature induced by the pump beam calculated at any r value. The thermal distribution through the length of laser rod for Gaussian and top hat heat source at steady state case are shown in figure(7) and figure (8) respectively.

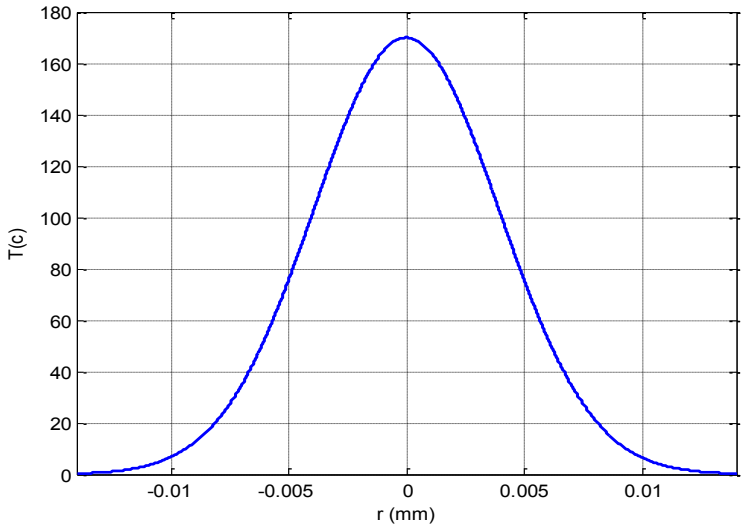

Figure (3) the relation between r and T.

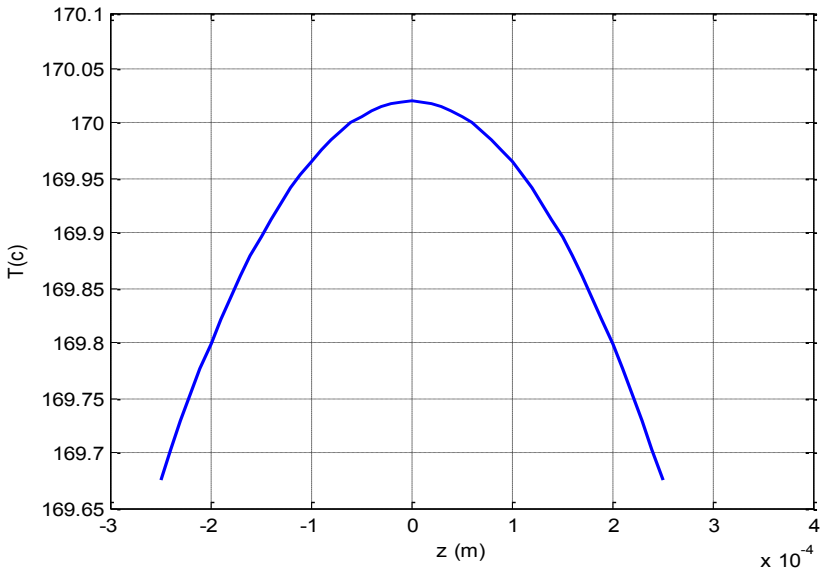

Figure (4) the relation between z and T.

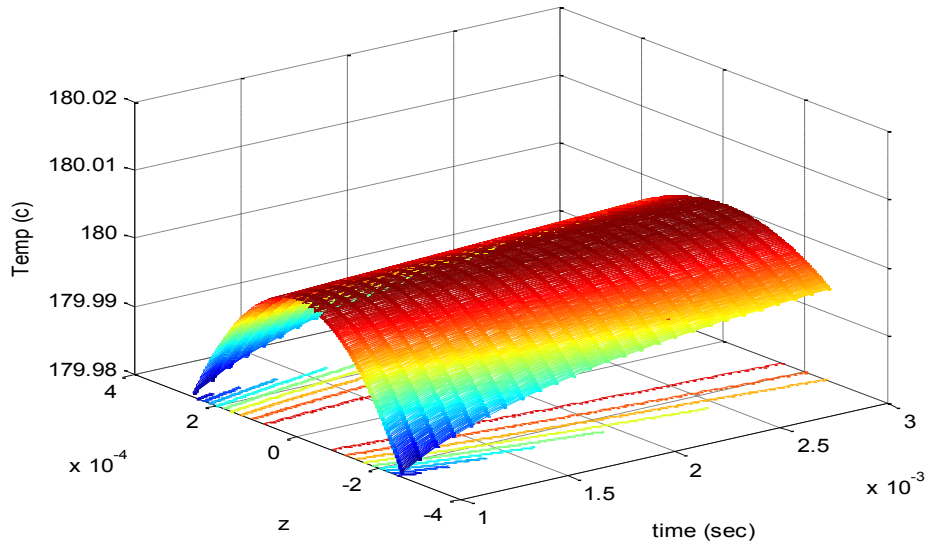

Figure (5) the time dependence of the temperature per unit volume induced by the pump beam calculated at any z value.

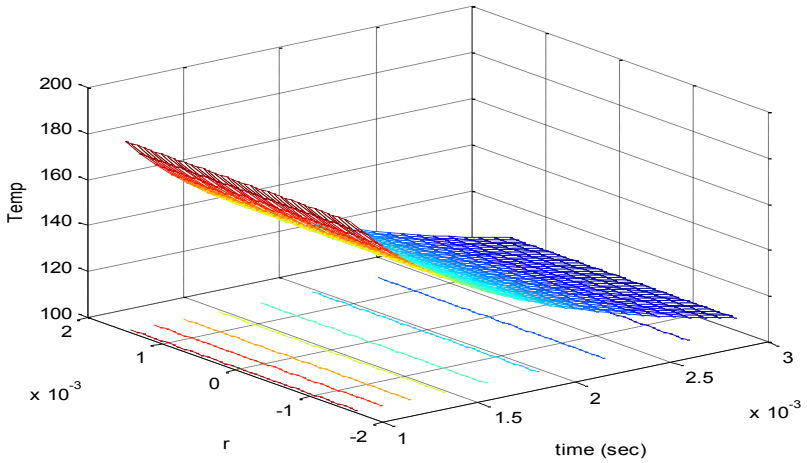

Figure (6) the time dependence of the temperature per unit volume induced by the pump beam calculated at any r value.

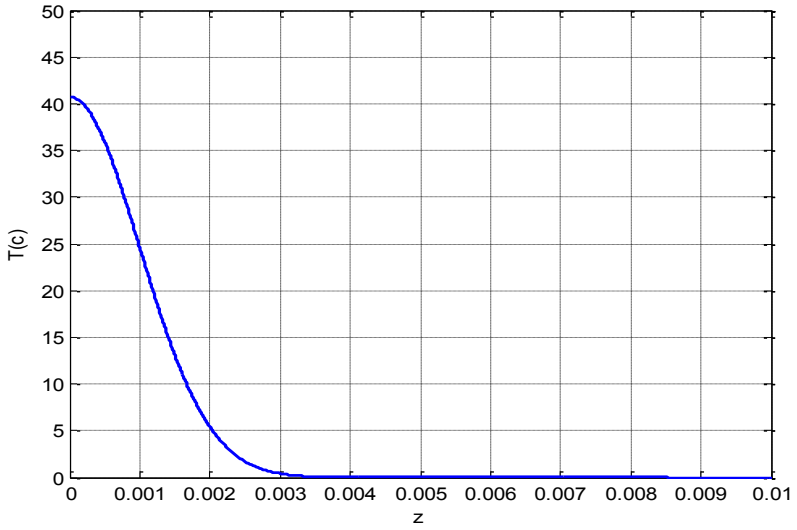

Figure (7) Thermal distribution through the length of the rod (z=250 μm) at Gaussian heat source.

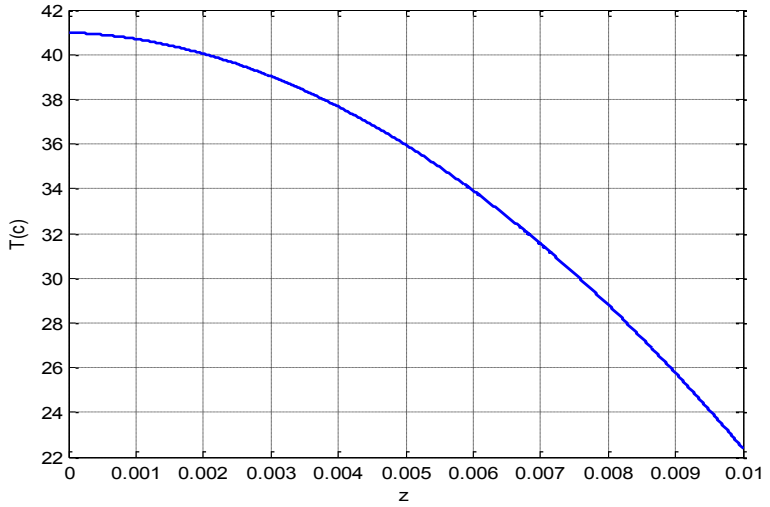

Figure (8) Thermal distribution through the length of the rod (z=250 μm) at Top hat heat source.

Using Bacterial Foraging Optimization Algorithm that allows simulating different cases of the laser rod heating by the continuous pumping with different space distributions of the pump power was developed. We use the algorithm to try to find the

minimum of the function in Figures (5 and 6) respectively. We assume that this surface can be sampled, but that the gradient is not known. The bacteria are initially spread randomly over the optimization domain. The results of the simulation are illustrated by motion trajectories of the bacteria on the contour plot of function in Figures (5 and 6) as shown in Figures (9 and 10) in the first generation, starting from their random initial positions, searching is occurring in many parts of the optimization domain, and we can see the chemotactic motions of the bacteria as the black trajectories where the peaks are avoided and the valleys are pursued. Reproduction picks the 25 healthiest bacteria and copies them, and then, as shown in Figures(9 and 10) in generation 2, all the chemotactic steps are in five local minima. This again happens in going to generations 3 and 4, but bacteria die in some of the local minima, so that in generation 3, there are four groups of bacteria in four local minima, whereas in generation 4, there are two groups in two local minima. Next, with the above choice of parameters, there is an elimination-dispersal event, and we get the next four generations shown in Figure s(10 and 11). Notice that elimination and dispersal shifts the locations of several of the bacteria and thereby the algorithm explores other regions of the optimization domain. However, qualitatively we find a similar pattern to the previous four generations where chemotaxis and reproduction work together to find the global minimum; this time, however, due to the large number of bacteria that were placed near the global minimum, after one reproduction step, all the bacteria are close to it (and remain this way). In this way, the bacterial population has found the global minimum. The final bacterial movement to explore the global minima is described in figures (12, a, b and c). The output power with change in incident pump power is given in figure (13). The output laser had a threshold of 18W. The maximum power output from the Yb:YAG laser was 22.5W for 80W of incident pump power. This gives an approximate slope efficiency of 52%.

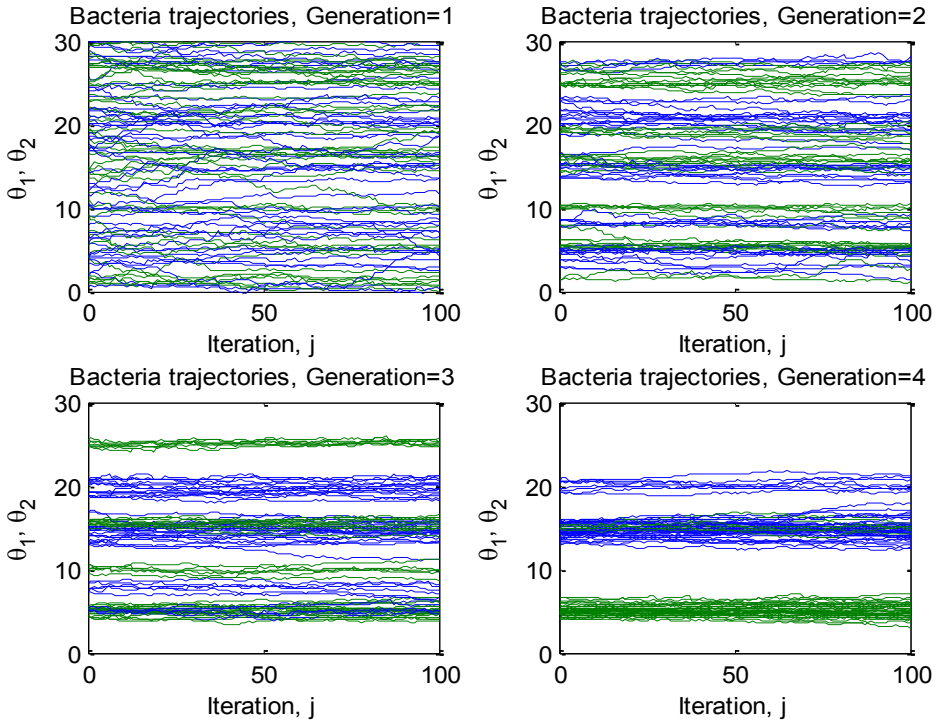

Figure (9) the motion trajectories of the bacteria on the contour plot of function in Figure (5).

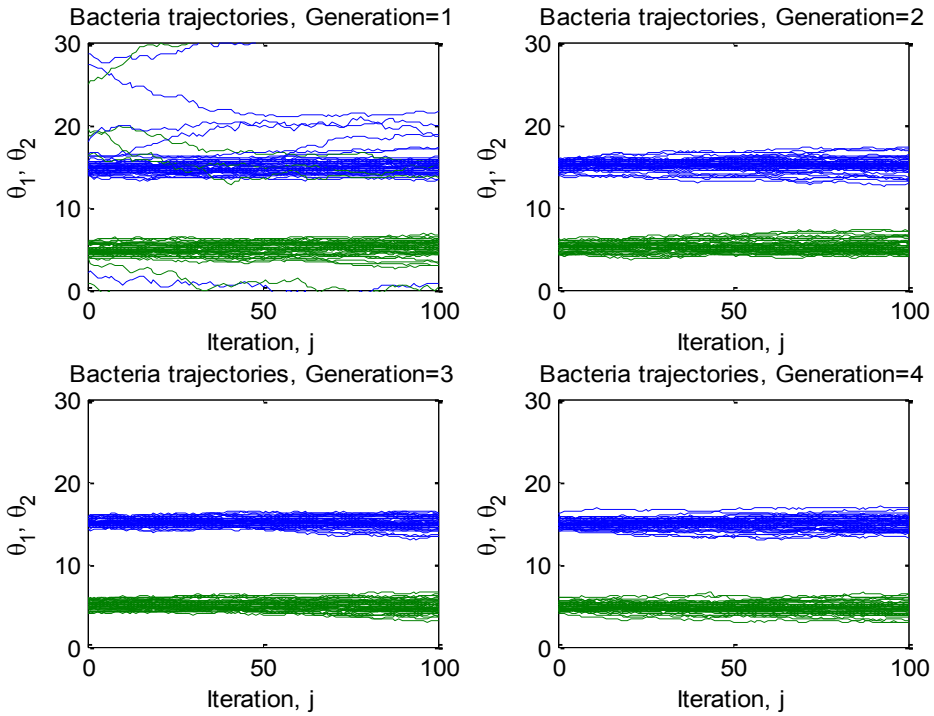

Figure (10) the motion trajectories of the bacteria on the contour plot of function in figure (6).

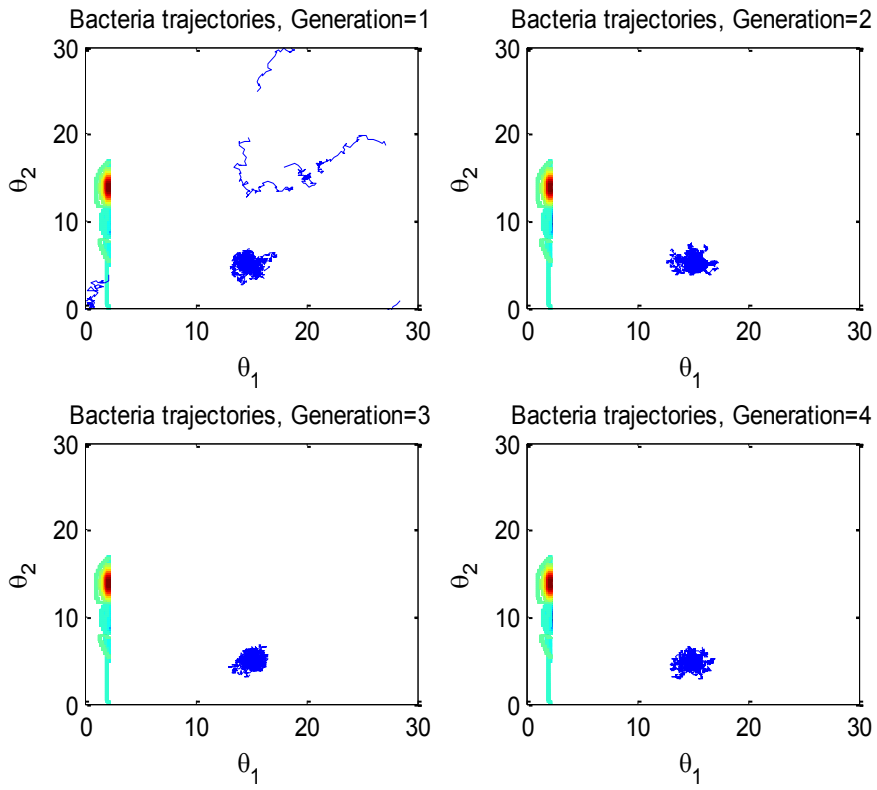

Figure (10) the algorithm explores other regions of the optimization domain for function in figure (5).

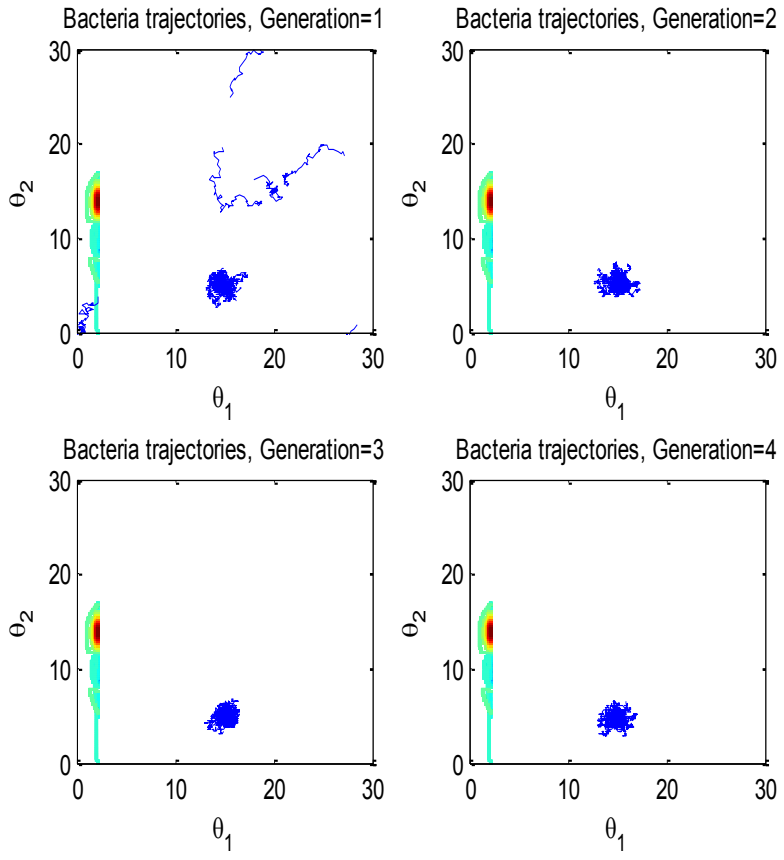

Figure (11) the algorithm explores other regions of the optimization domain for function in figure (6).

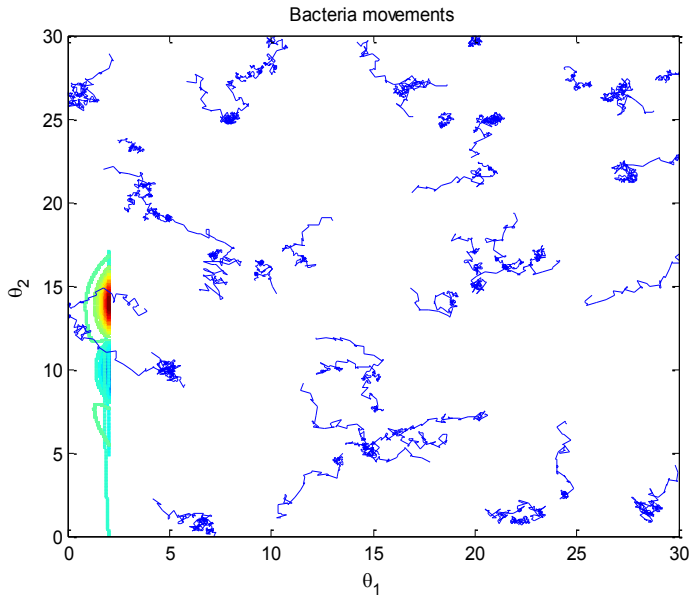

a- Bacterial movements

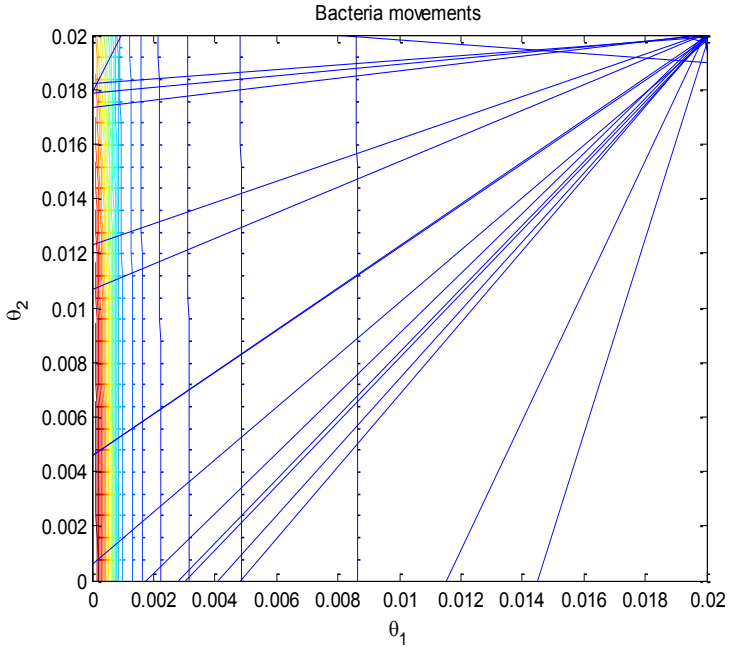

b- Bacterial movements

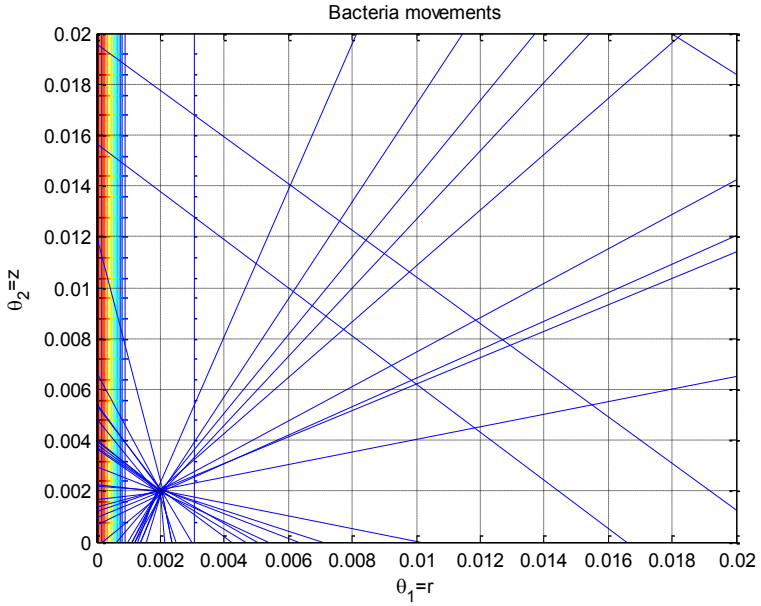

a- Bacterial movements

Figure (12) Bacterial movements through the serach space toward the global minima.

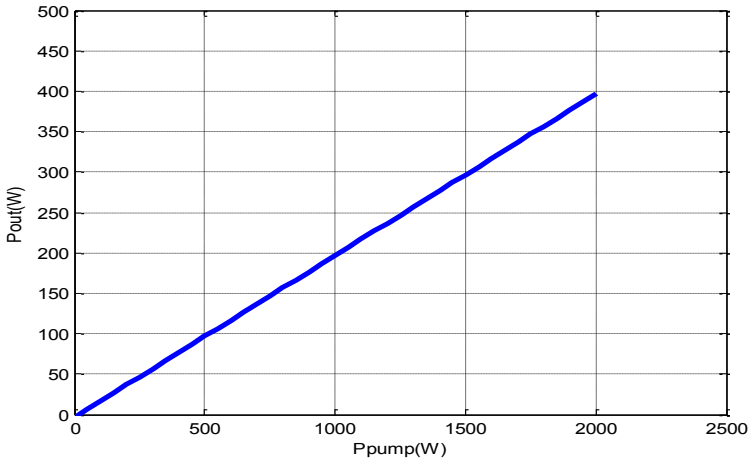

Figure (13) the output pump power from laser rod.

RESULTS AND DISCUSSION

Figures(3 and 4) show that Gaussian beam pumping will increase the temperature distribution more than that for Top hat beam especially, at the central portion of the rod. As the time of the irradiation increases the temperature increases and a greater gradient at r = 0 will build up. But because of the bad heat conductivity and the relatively small pulse duration the conducted energy remains small. This process lasts until the time at which the rate of the conducted heat energy into the cooler zones is equal to the rate of the energy of the absorbed radiation. At this time, the temperature reaches its maximum value after that the rate of the losses overcompensate the absorbed radiation and the temperature begins to decrease. Because of the great temperature gradient at the beginning of its reduction, the temperature decreases with a great slop followed by a smaller one till the end of the pump beam.

VALIDATION

The simulation found above will be compared with the results obtained by analytical solution. The validity of the analytical solution for thermal problems has been evaluated and confirmed in a reference [16] and can, therefore, is used as a reliable reference. Reference [16] reports on the validation of an analytical solution under the conditions which are considered in the present paper (cooling configuration, geometry, boundary conditions, shape of the pump beam along the transverse axis, etc.). Also in this reference experimental study was achieved, where the surface temperature of the disk is computed for various cases. One of these cases plots the surface temperature of the disk under a 500W heat load, when incorporating a heat sink. In order to verify the validity of this algorithm we proposed, experiment for The parameter of bacterial foraging optimization algorithm is as follows. We choose S =30, Ned =2, Nre =4 and Nc = 50. Is an implementation based on the description on the seminal work. We validate our model and the computational interpretation of swarms with algorithms implementing collision-based aggregation, collective perception, emergent taxis, foraging, and “random-tree” aggregation.

CONCLUSIONS

A new simulation algorithm modeling of the thermal problem in laser rods with circularly cylindrical symmetry was derived, taking in account an inhomogeneous heat source of the pumping beam along the propagation axis inside the laser rod. Comparison with analytical solution and FE simulations shows an excellent agreement. The BFOA method can be generalized to any cooling configuration as long as it has a circular symmetry. The heating function was assumed to have a Gaussian and Top hat transverse distribution but the proposed simulation method can be extended to many transversal shapes. In all practical cases, the solution of partial differential equations can be obtained in form of integrals, but in many cases these integrals are not easy to implement. The Bacterial Foraging Optimization Algorithm based on analytical expressions obtained for the temperature distribution open the way to a better physical

understanding of thermal phenomena and represent a fast tool for solid-state laser design and optimization. The same method can be implemented for obtaining the stress distribution and the thermally induced birefringence in heated laser rods.

REFERENCES

[1]. JABCZYÑSKI*, J.K. J. JAGUOE, W. ¯ENDZIAN, and J. KWIATKOWSKI, "Thermo-optic effects in solid state lasers end-pumped by fiber coupled diodes", Opto-Electron. Rev., Vol.13, No.1, 2005.

[2]. Boris A. Usievich, Vladimir A. Sychugov, Florent Pigeon, and Alexander Tishchenko, "Analytical Treatment of the Thermal Problem in Axially Pumped Solid-State Lasers", IEEE Journal of Quantum Electronics, Vol.37, No.9, Septemper, 2001.

[3]. Veysel Gazi and Kevin M. Passino, "Swarm Stability and Optimization", Springer Science + Business Media B.V. 2011.

[4]. Panigrahi,B.K. Y. Shi, and M.-H. Lim (Eds.), "Handbook of Swarm Intelligence: Concepts, Principles and Applications", Springer-Verlag Berlin Heidelberg, 2011.

[5]. Frank Träger, " Springer Handbook of Lasers and Optics", Springer Science+Business Media, LLC New York, 2007.

[6]. Orazio Svelto, "Principles of Lasers", Springer Science+Business Media, LLC 2010.

[7]. Clarkson :W.A. "Thermal effects and their mitigation in end-pumped solid-state lasers", J. Phys. D : Appl. Phys. 34 pp. 2381-2395, 2001.

[8]. El-Nicklawy, M. M. A. F. Hassan, El. M. A. Nasr, A.A. Hemida, S. L. Diab and S. M. El-Genedy, " Two Dimensional Temperature Distribution Resulting From Propagation of Light Beam Through Amplifying Medium", Egypt. J. Solids, Vol. (31), No. (2), 2008.

[9]. Dement'ev, A.S. A. Jovai.a, K. Ra_ckaitis, F. Ivanauskas, and J. Dabulyt_e-Bagdonavi_cien_e, "NUMERICAL TREATMENT OF THE TEMPERATURE DISTRIBUTION IN END-PUMPED COMPOSITE LASER RODS", Lithuanian Journal of Physics, Vol. **47**, No. 3, pp. 279.288 (2007).

[10]. Sychugov,V. A. V. A. Mikhailov, V. A. Kondratyuk, N. M. Lyndin, Y. Fram, A. I. Zagumennyi, Y. D. Zavartsev, and P. A. Studenikin, "Short wavelength (λ = 914 nm) microlaser operating on a Nd :YVO crystal," Quantum Electron., vol. 30, pp. 13–14, Jan. 2000.

[11]. Khalid S. Shaibib, Mohammed A. Minshid, Nebras E. Alattar, "Thermal and Stress Analysis in Nd:YAG Laser Rod with Different Double End Pumping Methods", Thermal Science, Vol. 15, 2011.

[12]. Jason Brownlee, "Clever Algorithms: Nature-Inspired Programming Recipes", Jason Brownlee., 2011.

[13]. Gopi, E.S. "Mathematical Summary for Digital Signal Processing Applications with Matlab", Springer Science+Business Media B.V. 2010.

[14]. Koji Sugioka, Michel Meunier, Alberto Piqu´e, "Laser Precision. Microfabrication", Springer-Verlag Berlin Heidelberg 2010.
[15]. Ashley J. Welch · Martin J.C. van Gemert, "Optical-Thermal Response of Laser-Irradiated Tissue", Second Edition ,Springer Science+Business Media B.V. 2011.
[16]. Vretenar,N. T. Carson, P. Peterson, T. Lucas, T. C. Newell, W. P. Latham, "Thermal and Stress Characterization of Various Thin-Disk Laser Configurations at Room Temperature", AFRL-RD-PS-TN, January, 2011.